Time-Space Asymmetry in (2+1) Causal Dynamical Triangulations

Maria Baryakhtar*
Harvard University
(Dated: October 8, 2009)

We present the results of numerical simulations of physical constants as a function of the scale and time-space asymmetry parameters in the framework of Causal Dynamical Triangulations in (2+1) dimensions. We focus on the properties of the model under symmetric and asymmetric scaling of simplices with respect to the time axis. We find that the uniform scaling parameter a has no effect on the physics of CDT other than setting the length units, and conclude that the scaling in this model is isotropic. In contrast, the α parameter which scales timelike but not spacelike lengths affects various aspects of the model. We report the results of changing the timelink lengths on bare constants Λ and G^{-1}, as well as develop a spacetime phase diagram that exhibits a nontrivial dependence on α under two distinct regimes. In addition, we present the α dependence of the time evolution of spacetime ensembles, measured using volume-volume correlators of the spacetimes. These suggest that changing α within the physical phase has effects other than simply scaling rate of time evolution which are not presently well-understood.

INTRODUCTION

Causal Dynamical Triangulations (CDT) is a discrete quantum gravity theory which seeks to describe spacetime through the basic principles of quantum mechanics. It was developed by Loll, Ambjorn, and Jurkeiwicz as a Lorentz variant on the largely unsuccessful Euclidean lattice theories [1]. The goal of CDT is to create a non-perturbative theory of the behavior of spacetime at all scales by calculating a gravitational path integral over geometries (i.e. metrics distinct under diffeomorphism) of spacetime. The calculations in 3 and 4 dimensions are performed almost exclusively numerically, through dynamical triangulation of discrete geometries. Dynamical triangulation, closely related to the Regge calculus method [2], provides a systematic method of approximating a spacetime with a discrete lattice, and of discretizing the corresponding action. The spacetimes are constructed with an explicit time dimension and a Lorentzian action.

The CDT approach has yielded promising results, including accurate dimensionality on large scales [3] and time evolution matching that of de Sitter space [4] even though a background geometry is never introduced into the computations. Additionally, unusual features have become apparent, such as a reduced spectral dimension on short scales, as well as quantum fluctuations on the emergent background spacetime which match analytic minisuperspace models [5]. This progress encourages futher investigation of the CDT model as a viable theory of quantum gravity.

We begin with a brief overview of Causal Dynamical Triangulations and the simulation methods; a more thorough description can be found in Zhang [6]. We present the results of investigating the space and time scaling behavior of the (2+1) dimensional theory, followed by a discussion of possible interpretations of the spacetime simulations.

BACKGROUND

Gravitational Path Integral

The path integral central to Causal Dynamical Triangulations is performed over the space of geometries, that is the space of smooth manifolds (spacetimes) with a fixed dimension and topology, and possessing a metric field tensor $g_{\mu\nu}$ [7]. The integral is only carried out over inequivalent geometries, such that diffeomorphisms of the same metric are not double counted. In analogy to the Feynman path integral, we integrate over the field degrees of freedom represented by $g_{\mu\nu}$:

$$G(g_0, g_1; t_0, t_1) = \int_{\frac{metrics}{diff}} \mathcal{D}g_{\mu\nu} e^{iS[g]} \tag{1}$$

where $S[g]$ is the standard Einstein-Hilbert action:

$$S[g_{\mu\nu}] = \frac{1}{16\pi G} \int d^n x \sqrt{-|g|}(R - 2\Lambda) \tag{2}$$

Numerical Calculations

The analytical analysis of Eqn. 1 is extraordinarily difficult and has not been fully carried out in 3 and 4 dimensions. A statistical approach has been developed in which the path integral is performed numerically using the Monte Carlo method. The integral can be discretized by triangulating the manifolds using dynamical triangulation, a more restricted form of Regge calculus in which edge lengths of the simplices are held fixed and the curvature is determined by the number of simplices which meet at a hinge [2].

There are two types of simplices from which the triangulations are constructed, pictured in Fig. 1.

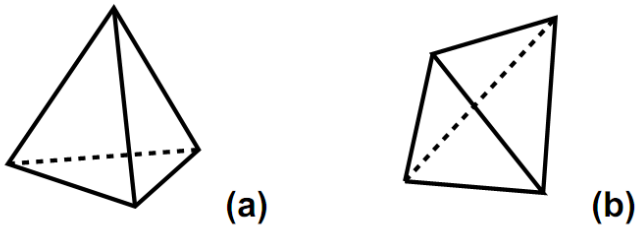

FIG. 1: The two simplex geometries in (2+1) dimensions, (3,1) (a) and (2,2) (b).

In constructing the spacetime lattice we enforce a causal structure by allowing only specific configurations of spacetime. We introduce a 'time' direction by splitting the spacetime into $(n-1)$-dimensional spacelike slices. This is visualized in Fig. 2. The simplices are labeled by the number of vertices in the two adjoining time slices. For example, a (3,1) simplex has three vertices in the t slice and one in the $t+1$ slice, while a (1,3) simplex is the inverse.

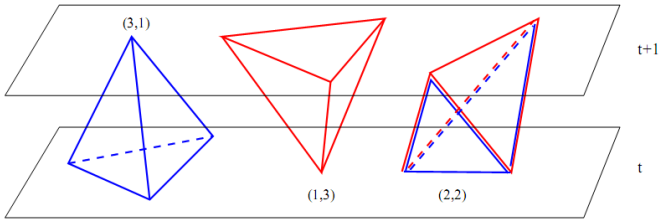

FIG. 2: Two timeslices at t and $t+1$ and three possible ways of fitting simplices in between.

From one time slice to the next, no topology change can occur; thus, this restriction prevents singularities of the metric and branching into 'baby-universes', which violate causality.

Using dynamical triangulations, we rewrite the continuum path integral (Eqn. 1) as a sum over inequivalent triangulations T:

$$Z = \sum_T m(T) e^{iS(T)} \tag{3}$$

where $m(T)$ is the measure on the space of triangulations. By applying the principles of Regge calculus, the continuous Einstein-Hilbert action (Eqn. 2) becomes

$$S[\mathcal{T}] = -k_0 N_0 + k_3 N_3 + k_t T \tag{4}$$

Here N_0 is the number of vertices, N_3 is the number of simplices, and T is the number of time slices. Constants k_0, k_3, k_t depend on the geometry of the simplices (volume and angles), as well as on fundamental constants Λ and G, the cosmological and Newton's constant, respectively.

To calculate the sum over the discretized triangulations, we perform a Wick rotation and rewrite the sum in Eqn. 3 as a partition function:

$$Z = \sum_T m(T) e^{iS_{Lorentz}(T)} \rightarrow Z = \sum_T m(T) e^{-S_{Euclidean}(T)} \tag{5}$$

This enables us to use Monte Carlo methods to perform the sum.

The moves used in the Monte Carlo sample the entire space of triangulations for a fixed topology; they are described in detail in [8]. The moves rearrange the geometry of the triangulation while preserving the topology and causal structure. These moves change the local curvature of the spacetime by splitting, combining, or rotating adjoining simplices - see for example Fig. 3.

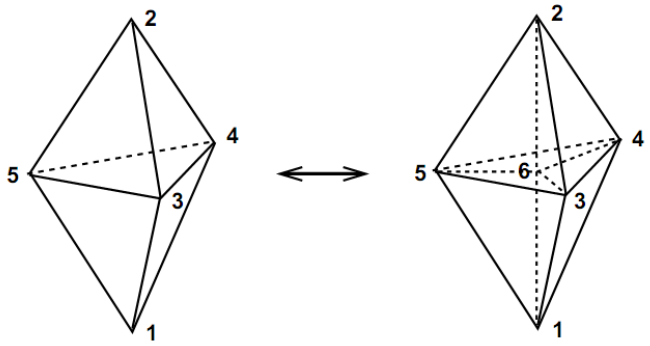

FIG. 3: The 2-6 move. A (3,1) and (1,3) simplex sharing a spacelike triangle are each split into three (3,1) simplices. This move adds one point and four simplices, incrementing N_0 by 1 and N_3 by 4, respectively. The inverse 6-2 move is also possible if the configuration on the right is present in the triangulation.

MOTIVATION: TIME-SPACE ASYMMETRY

In dynamical triangulations, the edge lengths of the simplices are kept fixed, and in most (2+1) simulations all the lengths have been set to 1 for simplicity [8]. In general, we can distinguish the spacelike link length $l_s^2 = a^2$ and the timelike link length $l_t^2 = -\alpha a^2$. Here a is the scale parameter, setting the overall 'size' of the simplices, and α is the asymmetry parameter that determines the ratio of time to space edge lengths.

While the calculations of the physical properties of the spacetime in (2+1) dimensions have been performed almost exclusively for $a, \alpha = 1$, the calculations in (3+1) have been performed for smaller values of α; in fact, it is

likely that in four dimensions the physical phase of the spacetime only appears for $\alpha < 1$. The motivation for this project was the investigation of the phase diagram in the (2+1) model as a function of α and a in connection to the (3+1) case presented in [5].

In general, investigating the asymmetry parameter addresses key questions. The crucial feature of CDT as compared to earlier Euclidean triangulation theories is the time axis, so it is important to understand the scaling of the time relative to the spatial dimensions and explain whether the time axis is solely preventing baby universe creation or has other effects on the structure of the resultant spacetime. Also we seek to test scaling properties of the spacetimes, which would probe questions of Lorentz invariance and the relation of CDT to anisotropic models.

The angles and volumes of simplices as functions of arbitrary a and α are derived in [7]. The general form of the action in $(2+1)$ dimensions is [1]:

$$\begin{aligned} S[\mathcal{T}] &= (4ak(K_1 - K_2) - 4a^3\lambda(L_1 - L_2))N_0 \\ &+ (ak \cdot K_2 - a^3\lambda \cdot L_2)N_3 \\ &+ (4ak(-\pi\sqrt{\alpha} - 2(K_1 - K_2)) + 8a^3\lambda(L_1 - L_2))T \end{aligned} \tag{6}$$

where the constants K_1, K_2, L_1, L_2 in the action are functions of α only:

$$\begin{aligned} K_1 &= \pi\sqrt{\alpha} - 3\text{arcsinh}\frac{1}{\sqrt{3}\sqrt{4\alpha+1}} - 3\sqrt{\alpha}\arccos\frac{2\alpha+1}{4\alpha+1} \\ K_2 &= 2\pi\sqrt{\alpha} + 2\text{arcsinh}\frac{\sqrt{8(2\alpha+1)}}{4\alpha+1} - 4\sqrt{\alpha}\arccos\frac{-1}{4\alpha+1} \\ L_1 &= \frac{\sqrt{3\alpha+1}}{12} \\ L_2 &= \frac{\sqrt{2\alpha+1}}{6\sqrt{2}} \end{aligned} \tag{7}$$

In the construction of the Wick rotation, the $(2, 2)$ simplices degenerate at $\alpha = 1/2$, that is their volume goes to 0 [7]. Thus the method of approximating the action via Monte Carlo breaks down for values of α of $1/2$ and smaller. In the following analysis, we consider a representative range of values of α from 0.51 to 10.0 and a from 0.6 to 2.0; these were found to be representative and excepting $\alpha \leq 0.5$ no changes in behavior of the model are observed or expected outside of these values.

SIMULATION PROCEDURE

In order to perform calculations, we must set the number of time slices T and total volume V of the spacetime. Larger volumes are usually more accurate due to finite size lattice effects; however, large volumes are very computationally expensive. We use $V = 16,000$ and $V = 32,000$ depending on the calculation.

For each simulation, we set the geometry of the simplices, which is determined by the parameters a and α:

$$l_s^2 = a^2 \qquad l_t^2 = -\alpha a^2 \tag{8}$$

where l_s and l_t are the spacelike and timelike link lengths, respectively. Here, a has dimensions of length and α is dimensionless.

In addition we set the fundamental constants which enter the action. We denote $k = 1/(8\pi G)$, where G is the bare gravitational constant, and $\lambda = k\Lambda$, where Λ is the bare cosmological constant.

Each time slice has S^2 topology, though we should emphasize that no background geometry is set or assumed. We impose periodic boundary conditions (S^1 topology) on the time direction for ease of calculation. The initial configuration of the spacetime is the minimal triangulation of the $S^1 \times S^2$ topology.

In order to perform measurements of physical observables of the spacetime, we must take an ensemble average over many sweeps (a sweep is defined as V attempted Monte Carlo moves, where V is the total volume); a single sweep is interpreted as a quantum fluctuation of the spacetime itself, with no direct physical interpretation. Thus we measure observables as an average over many sweeps. Before performing any calculations, we first thermalize the spacetime, that is perform on the order of $100,000$ random sweeps so the starting configuration is randomized and not dependent on the artificial initialization of the spacetime.

RESULTS

Bare Constants: α Dependence

In order for the state sum to converge in the first place, we have to tune the bare cosmological constant λ to its critical value $\lambda_c(k)$ to obtain a continuum limit [8]. The critical value of the cosmological constant is a function of the inverse bare gravitational constant $k = \frac{1}{8\pi G}$ [8]. For values of λ above the critical, the spacetime quickly shrinks to a minimal value, and for λ below the critical value, the sum diverges and the volume grows exponentially as the simulation runs. Since the system is very sensitive to changes around this critical value, we introduce an extra term in the action $\delta S = \epsilon|N_3 - N_3^{init}|$, with $\epsilon \ll 1$, which keeps the volume roughly constant and the sums from diverging in a finite neighborhood of λ_c without affecting the dynamics. For the purposes of the simulation we find $\epsilon = 0.02$ to be a well-suited value.

As a first step to studying the effect of tuning the asymmetry parameter α on the spacetime we look at the behavior of the $\lambda_c(k)$ curve as a function of α. For these

measurements, the scale parameter a is held fixed at 1. The results for representative values of α from 0.6 to 10 are shown in Fig. 4.

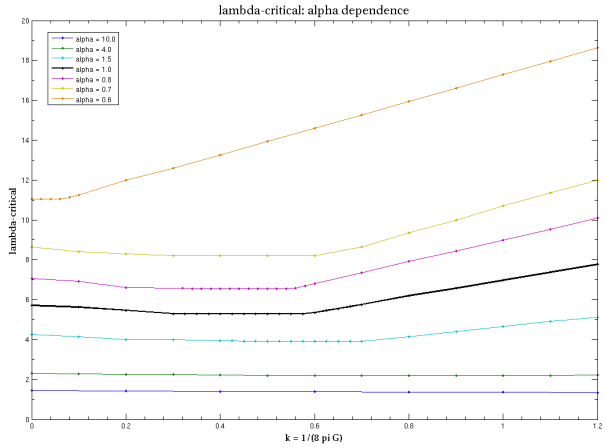

FIG. 4: Critical values of bare constant λ as a function of k, for different values of the time-space asymmetry α.

The λ_c curves were calculated using code that steps through values of k and loops through corresponding values of λ, evaluating the behavior of the spacetime in terms of whether the volume is diverging or collapsing (See Appendix). If the volume stays constant to a specified precision, over a given number of sweeps, the current value of λ is accepted as λ_c. In the simulations presented here, the precision used was 5% or less over 2000 moves. For the purposes of this simulation, we use a relatively small spacetime (volume $V = 16,000$, number of timeslices $T = 16$) for speed of calculation. Sample values for larger spacetimes were found to be consistent with these results.

Phase Transition

Spacetimes with constants tuned to give the continuum limit do not always result in a physically significant spacetime geometry. For $\alpha, a = 1$, two distinct phases of the spacetime exist, 'extended' physical phase at small k and the 'decoupled', or unphysical, phase at large k [8]. A visualization of the phases is presented in Fig. 5, where the horizontal axis represents the time slice and the radial direction represents the spatial volume at that slice. In the decoupled phase, multiple separate slices like the one shown in Fig. 5(b) can appear and evolve independently of one another. In the extended phase, neighboring slices are strongly coupled. Note that the three dimensional figures are rendered for ease of visualization only; the individual spacetimes are not necessarily rotationally symmetric about the time axis.

The two phases can be quantitively distinguished by

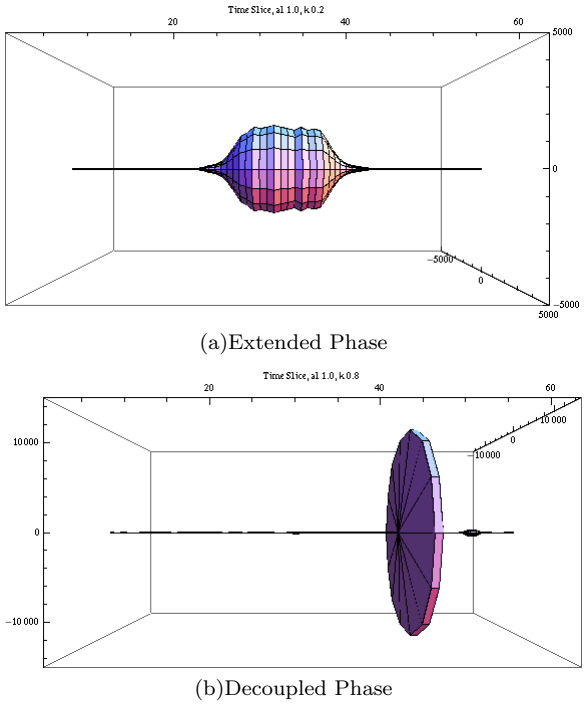

(a)Extended Phase

(b)Decoupled Phase

FIG. 5: The two phases of spacetime in (2+1) dimensions. In the decoupled phase, multiple separate slices like the one shown in (b) can appear and evolve independently of one another. In the extended phase, neighboring slices are strongly coupled (a). These spacetimes were generated at $T = 64$ and $V = 32,000$. At larger volumes, more visible slices often appear in the decoupled phase.

calculating the ensemble average of the order parameter $P = N_{22}/N_3$, the number of (2,2) simplices divided by the total number of simplices in the spacetime. For spacetimes in the extended phase, P is a finite value between 0 and 1 (generally between 0.3 and 0.5). As the value of k increases, the spacetime transitions to the decoupled phase and the value of the order parameter drops to $P \approx 0$. In this and subsequent results, as we change the value of k, we change λ as well to keep it at the critical value $\lambda_c(k)$; otherwise the spacetime becomes ill-defined.

α Dependence

The phase transition point in k was studied as a function of α by calculating the point where the order parameter drops to 0. The results are plotted in Fig. 6. At $\alpha \approx 0.75$, the phase transition occurs at a minimum value of $k = 0.525 \pm 0.025$. For $0.5 < \alpha < 0.75$ and $\alpha > 0.75$, the transition occurs at higher values of k.

In these measurements, the spacetimes were generated at volume $V = 16,000$ and $T = 16$ time slices. Each point in the order parameter plot was calculated on thermalized spacetimes (50,000 initial sweeps) and averaged

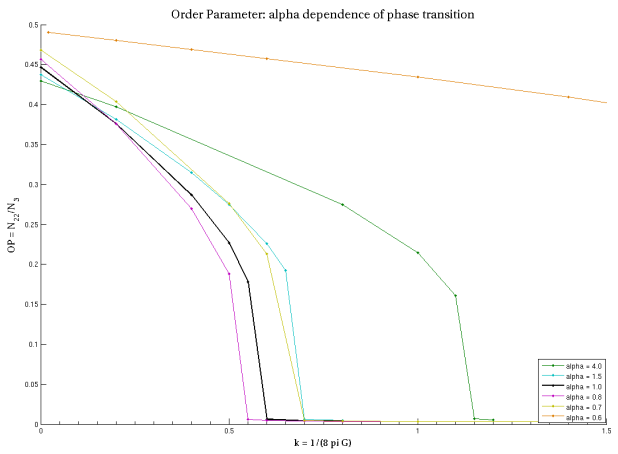

FIG. 6: The phase transition as measured by the order parameter. The phase transition occurs at different points depending on the value of α.

over 50,000 sweeps. Running the simulation at higher spacetime volume or longer thermalization sweeps did not affect the results.

The results can be summarized in a phase diagram as a function of α and k as seen in Fig. 7.

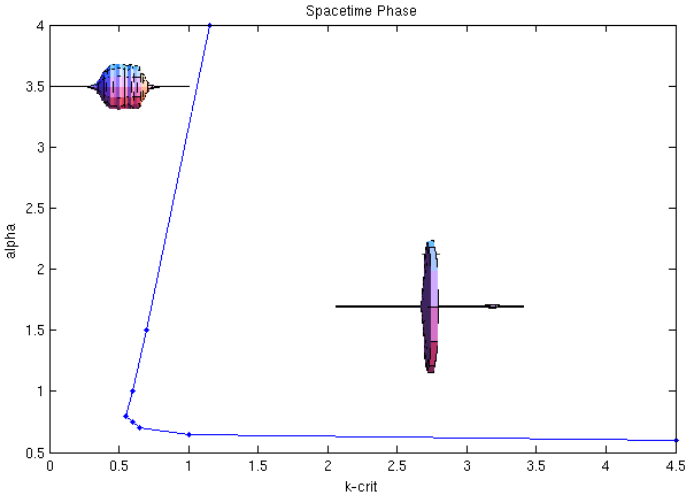

FIG. 7: The transition between the two spacetime phases depends on both k and α. The value of λ is set to $\lambda_c(k)$ as k is varied.

a Dependence

A similar measurement was carried out to investigate the order parameter dependence on the overall scale parameter a. While α is dimensionless, a has units of length, so to see whether the phase transition depends on a in an essential way, we plot the order parameter P against the dimensionless quantity $k \cdot a$ (Figure 8). The transition takes place at the same point $ak = 0.575 \pm 0.05$ for a varying between 0.6 and 2.0. Here $\alpha = 1$ for all curves.

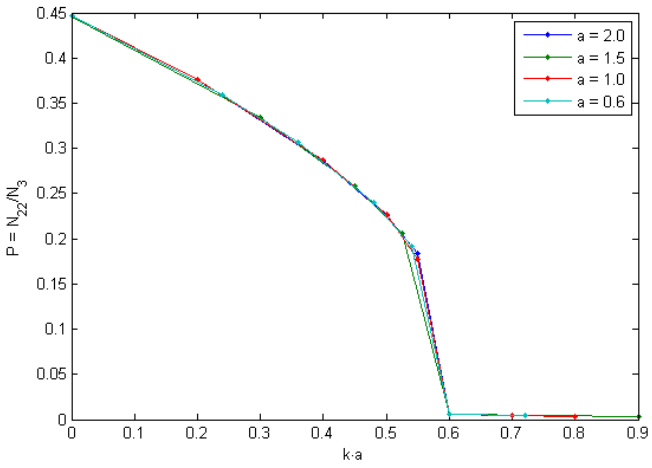

FIG. 8: The phase transition measured through the order parameter. The transition takes place at the same point $ak = 0.575 \pm 0.05$ for a varying between 0.6 and 2.0. Here $\alpha = 1$ for all curves.

Volume-Volume Correlator: α Dependence

To get an understanding of the time evolution of the spacetime ensemble, we use the volume-volume correlation function $C(\Delta)$[6]:

$$C(\Delta) = \frac{1}{T^2} \sum_{t=1}^{T} \langle N_2(t) N_2(t+\Delta) \rangle \qquad (9)$$

where T is the total number of time slices and N_2 is the spacelike volume of the slice at time t. The volume-volume correlator was measured for a range of spacetimes for different values of α. The behavior of the volume-volume correlator function is dependent on the value of k [8], so for consistency all the simulations were performed at $k = 0.2$, which falls in the extended phase of the spacetime for all the relevant values of α.

As this calculation is more sensitive to spacetime size, we use $V = 32,000$ and $T = 64$. The spacetimes are thermalized for 200,000 sweeps and the measurement is taken as an average over a sample of 200 spacetime fluctuations out of 100,000 sweeps. The results are shown in Fig. 9.

The data is fitted to the time evolution of the de Sitter solution to Einstein's equation in 3 dimensions, $t \propto \cos^2(Ht)$ where H is Hubble's constant (the solution is Wick rotated to match the Euclidean method

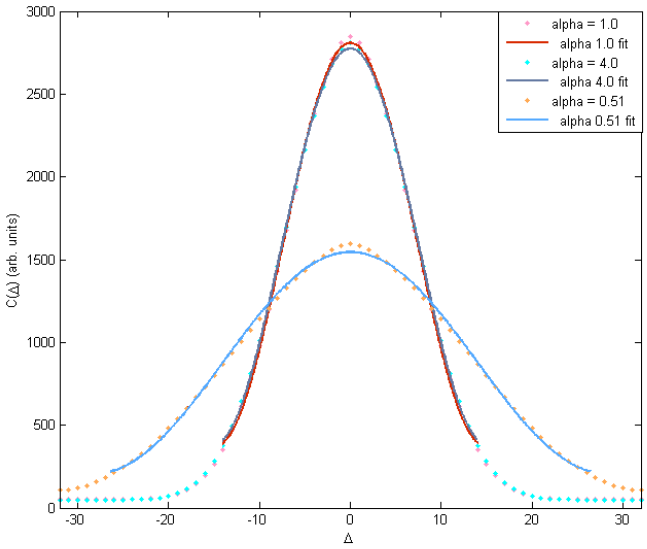

FIG. 9: Volume-volume correlator function for different values of α. The data is fitted to the time evolution of a de Sitter solution to Einstein's equation, $t \propto \cos^2(Ht)$.

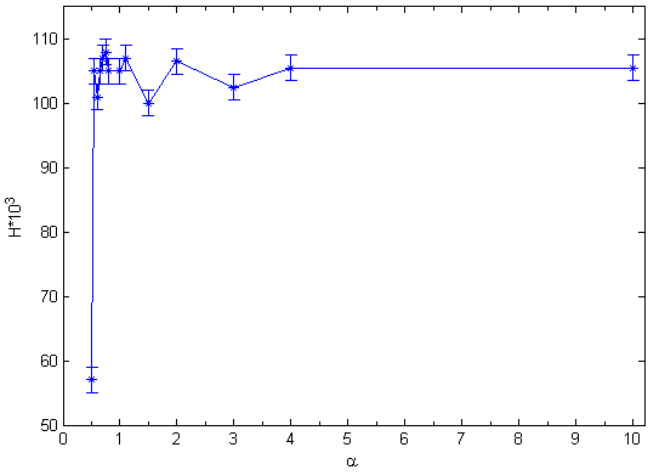

FIG. 10: Hubble constant H, derived as a fit parameter of the time evolution of spacetimes at different α values. Error bars represent the 95% condifence interval on the fit parameter.

of computing CDT sums) [4]. The fit parameter H is then plotted against α in Fig. 10. In the simulations, the extended spacetime is confined to a part of the time axis and surrounded by 'stalks' of minimal spatial extent (see Fig. 5(a)). As the 'stalk' is not part of the physical evolving spacetime, we exclude it by restricting the fits to the top 90% of $C(\Delta)$ values. The fits have R-squared values > 0.999 and the error bars represent the 95% condifence interval on the fit parameter. Values of H for independent spacetimes with equivalent parameters agree to within the fit precision.

DISCUSSION

Bare Constants: α Dependence

There is a clear dependence of the $\lambda_c(k)$ curve on α (Fig. 4): as α increases from 1 to 10, the values of λ decrease and the curve becomes more shallow. As α decreases toward $\alpha = 0.51$, λ_c increases sharply, especially at higher k. This behavior is consistent with the curvature of spacetime changing as α varies. The connection between α and λ_c can be understood as follows: the background spacetime which emerges from the CDT calculations closely resembles the fully symmetric solution to Einstein's equations, a 3-sphere with radius $R \propto \Lambda_{eff}^{1/2}$. Thus constraining the volume of the spacetime as we do for the purposes of the simulation is equivalent to setting the effective cosmological constant $\Lambda_{eff} \propto V^{-2/3}$.

At the same time, changing α changes the volume of the simplices, thereby changing the volume of the spacetime. The volumes of the (3,1) and (2,2) simplices both scales as $\sqrt{\alpha}$ [7]:

$$Vol(3,1) = \frac{1}{12}\sqrt{3\alpha+1}$$
$$Vol(2,2) = \frac{1}{6\sqrt{2}}\sqrt{2\alpha+1} \qquad (10)$$

so lowering α will decrease the spacetime volume and increase the effective cosmological constant. We emphasize here that the constant λ in the action and the simulations is proportional to the bare cosmological constant and cannot be directly compared to Λ_{eff}; however, there is a relationship between the effective constant and continuum limit value λ_c that is clearly demonstrated by the λ_c dependence on α.

Phase Transition

In order to calculate the phase transition point we use the order parameter $P = N_{22}/N_3$. It is not clear whether the order parameter should have any continuum limit interpretation, but it has been found to accurately describe the transition between the extended and the decoupled phase [8]. This parameter can be intuitively understood as follows. The (3,1) and (1,3) simplices are effectively triangulations of the 2-dimensional spacelike slices, with only a point in the next slice (see Figure 1). Thus, the way that spacelike surfaces can be triangulated with the bases of (3,1) simplices is independent of the triangulations of the surrounding time slices. The (2,2) simplices, on the other hand, connect neighboring time slices. At

low counts of (2,2) simplices, the (3,1) simplices dominate and the spacelike surfaces become decoupled from each other as separate 2-dimensional triangulations that evolve independently. This corresponds to the decoupled phase, which has order parameter $P = N_{22}/N_3 \approx 0$. For higher values of N_{22}, the slices become coupled through (2,2) simplices, and the spacetime shifts into the extended phase. For a more detailed analysis, see [8].

α Dependence

As seen from the phase diagram Fig. 7, there are two phases that appear for a range of k and α values. These phases are qualitatively equivalent to the decoupled and extended phases which exist at $\alpha = 1$. We find no third phase for other α values, in contrast to the results in (3+1) dimension where three phases were found, and the physical extended phase was only present for $\alpha < 1$ [5]. This result is understandable, as the third phase in 4 dimensions was unphysical and may be an artifact of the lattice approximation that only occurs in higher dimensions.

We do observe an interesting feature of the diagram, which possesses two distinct regions. For $\alpha < 0.75$, the dependence on k of the phase transition is very steep: for $\alpha = 0.7$ the transition from the extended to the decoupled phase takes place at $k = 0.675 \pm 0.025$, where as for $\alpha = 0.6$, the critical value is $k = 4.05 \pm 0.05$. On the other hand, for $\alpha > 0.75$. the critical value of k decreases very slightly with descreasing α.

We consider whether the value $\alpha = 0.75$ is of mathematical significance in the action. Since the phase structure is closely related to the order paremeter $P = N_{22}/N_3$, we choose to rewrite the expression for the action (Eqn. 4) as

$$S[\mathcal{T}] = k_{22}N_{22} + k_{31}N_{31} + k_1 N_1 \qquad (11)$$

where N_{22} is the number of (2,2) simplices and N_{31} the combined number of (3,1) and (1,3) simplices, and k_{22}, k_{31} are the corresponding constant coefficients [7]. Calculating the relative ratio of the coefficients provides information about the relative importance of each type of simplex in the action as a function of α. The result is shown in Fig. 11.

With respect to the action, the value $\alpha = 0.75$ is indeed special, where it represents a transition between two regimes: at small α, where the weight of (2,2) simplices in the action is rapidly growing, and at large α, where the importance of (2,2) simplices is slowly decreasing. These two behaviors may explain the two distinct regions of the spacetime phase diagram that are apparent.

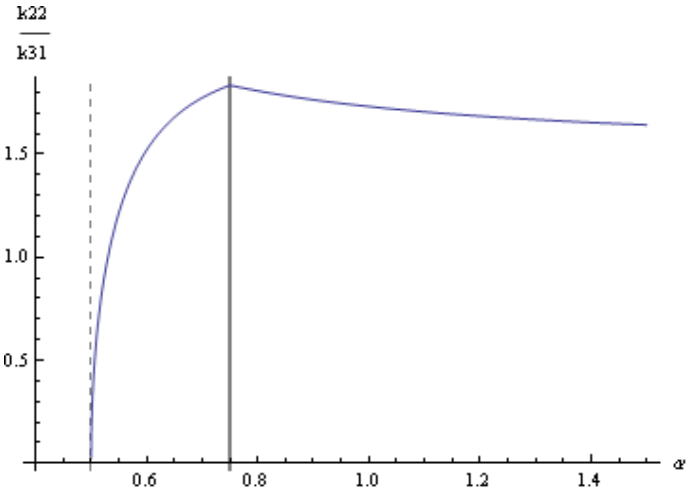

FIG. 11: k_{22}/k_{31}, representing the relative weights of $(2,2)$ *vs.* $(3,1)$ simplices in the action as a function of α. The functional behavior changes at $\alpha = 0.75$, denoted by the vertical line.

a Dependence

We find that the phase transition as a function of the dimensionless quantity $k \cdot a$ is independent of a, the length of the edges. The transition takes place at $ka = 0.575 \pm 0.05$ independent of the value of a. Judging from the phase transition, we conclude that the scaling of the spacetime in CDT is isotropic.

Volume-Volume Correlator: α Dependence

The dependence of the Hubble constant on α (Fig. 10) can be split into two distinct regions similar to the phase diagram dependence. At $\alpha \gtrsim 0.75$, H remains approximately constant within the fit precision. This suggests that for $\alpha > 0.75$, the time-space asymmetry acts simply as a scaling factor, stretching the simlpices in the time direction. However, for $\alpha < 0.75$, the Hubble constant is strongly dependent on alpha, increasing by nearly a factor of two between $\alpha = 0.51$ and $\alpha = 0.6$. This may indicate a different physical regime, or the breakdown of the model as we approach the degenerate value $\alpha = 0.5$. In either case, this result is very important to understanding the physical interpretation of the CDT theory.

CONCLUSION AND FUTURE WORK

We present the results of studying the dependence of the $2+1$ CDT model on two scaling factors, a and α. By calculating the phase transition points between physical and decoupled spacetime regions, we conclude that the spacetime is invariant under scaling of a, and that the

model is isotropic.

The phase diagram with respect to the time-space asymmetry parameter α contains two distinct regimes, $\alpha < 0.75$ and $\alpha > 0.75$. We expect that the two regions of the phase diagram result from the interaction of (2,2) and (3,1) simplices in the triangulation, as the behavior of the relative weights of the simplices changes at the transition point $\alpha = 0.75$.

In addition, we find an interesting scaling of the time evolution of the spacetimes as a function of the α parameter. Again, we note two different regimes, separated by $\alpha = 0.75$. While for large α, the parameter the evolution in time is approximately constant, at large α the dependence is non-trivial and remains to be interpreted. The data can be improved by running simulations at higher spatial volumes and numbers of time slices. Acquiring more precise data points is very important to reaching conclusive results for time axis scaling and the H vs. α dependence, both at high and low α. Understading the properties of the different regions of the model in α is crucial to interpreting the triangulations as physical spacetime fluctuations, and judging the role of the time axis in Causal Dynamical Triangulations.

Acknowledgements

This work would not be possible without many fascinating conversations with Professor Steven Carlip and his support and guidance, as well as the help of graduate students Rajesh Kommu and Michael Sacks. The project was funded by NSF through the UC Davis REU program.

* mbaryakh@fas.harvard.edu

[1] J. Ambjorn, J. Jurkiewicz, and R. Loll, Phys.Rev.Lett. **85**, 924 (2000), [arXiv:hep-th/0002050v3].
[2] R. M. Williams, Class. Quantum Grav. **9**, 1409 (1991).
[3] J. Ambjorn, J. Jurkiewicz, and R. Loll, Phys.Rev.Lett. **95**, 171301 (2005), [arXiv:hep-th/0505113v2].
[4] J. Ambjorn, J. Jurkiewicz, and R. Loll, Int.J.Mod.Phys **D17**, 2515 (2009), [arXiv:0806.0397v2 [gr-qc]].
[5] J. Ambjorn, J. Jurkiewicz, and R. Loll, Phys.Rev. D **72**, 064014 (2005), [arXiv:hep-th/0505154v2].
[6] J. Zhang, Davis REU Final Report (2007).
[7] J. Ambjorn, J. Jurkiewicz, and R. Loll, Nucl.Phys.B **610**, 347 (2001), [arXiv:hep-th/0105267v1].
[8] J. Ambjorn, J. Jurkiewicz, and R. Loll, Phys.Rev.D **64**, 044011 (2001), [arXiv:hep-th/0011276v2].

```
;;runlambda.lisp
;;Masha Baryakhtar, August 17, 2009

;; some code-specific parameters
(defparameter *lambda-step* 0.01)
(defparameter *BIG* 1000)
(defparameter *precision* 0.05)
(defparameter *hi-bound* 1.5)
(defparameter *lo-bound* 0.6)
(defparameter *T* 16)
(defparameter *lambda-c* 2.68)

;;;;;;;;;;;;;;;;;;;;;;;;;;;;;;;;;;;;;;;;;;;;;;;;;;;;;;;;;;;;;;;;;;;;;;;;;;;;;;;;;;;;;;;;;;;;;;;;
;; load all the main files
(load "/home/baryakhtar/Documents/cdt-common-lisp/2plus1/load-files.lisp")

;;;;;;;;;;;;;;;;;;;;;;;;;;;;;;;;;;;;;;;;;;;;;;;;;;;;;;;;;;;;;;;;;;;;;;;;;;;;;;;;;;;;;;;;;;;;;;;;
;; set starting constants

(setf eps 0.02)
(setf NUM-SWEEPS 2000)
(setf SAVE-EVERY-N-SWEEPS (/ NUM-SWEEPS 10))

(format t "*** Set constants ***. ~%
eps = ~A kk = ~A lambda = ~A alpha = ~A a = ~A NUM-SWEEPS = ~A SAVE-EVERY-N-SWEEPS = ~A~2%"
        eps kk llambda alpha a NUM-SWEEPS SAVE-EVERY-N-SWEEPS)

;;;;;;;;;;;;;;;;;;;;;;;;;;;;;;;;;;;;;;;;;;;;;;;;;;;;;;;;;;;;;;;;;;;;;;;;;;;;;;;;;;;;;;;;;;;;;;;;
;; prints out spacetime size to screen
;; used for tuning the kk and lam parameters (runlambda.lisp)
;; return 1 for exploding (lambda too low), -1 for collapsing(lambda too high)
;; and 0 if on lambda-c

(defun generate-spacetime-data-console (&optional (start-sweep 1))
  (let* ((end-sweep (+ start-sweep NUM-SWEEPS -1)) (totsimp 0.0) (avg 0.0))
    (do ((ns start-sweep (1+ ns))) ((> ns end-sweep))
      (sweep)
      (when (= 0 (mod ns SAVE-EVERY-N-SWEEPS))
        (format t "start = ~A end = ~A current = ~A count = ~A~%"
                start-sweep end-sweep ns (count-all-types))
        (format t "** avg = ~A **~%" avg)
        )

      ; if simplex count too far from initial value, lambda is not at lambda-c.
      ; return 1 for too big, -1 for too small
      (when (> (N3) (* N-INIT *hi-bound*))
        (return-from generate-spacetime-data-console 1))

      (when (< (N3) (* N-INIT *lo-bound*))
        (return-from generate-spacetime-data-console -1))

      ; divide by 1000 to keep numbers small. keep track of avg spacetime size
      ; weigh average by sweep number to make later sweeps matter more
      (incf totsimp (/ (* (N3) ns) *BIG*) )
      (setf avg (/ totsimp (/ (+ ns (expt ns 2)) 2)))


      ; if average gets too far from initialized value, return 2 for lambda too small
      ; -2 lambda too small. only test after some number of sweeps b/c in the beginning
      ; size tends to fluctuate a lot, esp toward low numbers
      (when (> (* avg *BIG*) (* N-INIT 1.15))
        (return-from generate-spacetime-data-console 2))
      (when (and (> ns (/ end-sweep 4)) (< (* avg *BIG*) (* N-INIT 0.7)))
        (return-from generate-spacetime-data-console -2))
```

```lisp
          (if (= ns end-sweep)
            ;; if code running too long, increase tolerance by 1% to prevent getting stuck
            (if (> end-sweep (* NUM-SWEEPS (* *precision* 100)))
                (incf *precision* 0.01)

                ; on last sweep, if size fluctuations are too big (>precision%), add more iterations
                (if (> (abs (- (* avg *BIG*) N-INIT)) (* N-INIT *precision*))
                    (incf end-sweep NUM-SWEEPS)
                    )
                )
            )


      ))
; if successful return 0
  0
)

;;;;;;;;;;;;;;;;;;;;;;;;;;;;;;;;;;;;;;;;;;;;;;;;;;;;;;;;;;;;;;;;;;;;;;;;;;;;;;;;;;;;;;;;;;;;;;;;;;;;
;; runs over lambda values and returns lambda-c for a given kk
(defun calc-lambda (&key (a 1.0) (alpha -1.0) (kk 0.0) (llambda 0.0))
  (let* ((st 0) (kkcurr kk) (lambda-curr llambda))

  ;; calculates the action coefficients (for monte-carlo.lisp) to speed up computation.
  ;; has inputs of link lengths and fundamental constants
  (calculate-action-coeff :a a :alpha alpha :kk kkcurr :llambda lambda-curr)

  ;; redefine spacetime to clear it-otherwise will throw error each time
  (setf *spacetime* (make-hash-table :size 8192))

  ;; initialize spacetime
  (initialize-t-slices-with-v-volume :num-time-slices *T* :target-volume (* *T* 1000)
                                     :boundary-conditions 'periodic :spatial-topology 'S2)

  ;; runs monte carlo and outputs spacetime size to screen
  (setf st (generate-spacetime-data-console))

  (format t "*** st = ~A ***~2%" st)

  ;; increments lambda up or down until spacetime size stays constant
  (if (> st 0)
      (calc-lambda :a a :alpha alpha :kk kkcurr :llambda (+ lambda-curr *lambda-step*))
       ;else
      (if (< st 0)
          (calc-lambda :a a :alpha alpha :kk kkcurr :llambda (- lambda-curr *lambda-step*))
          (if (= st 0) lambda-curr)
          )
      )
   )
)
;;;;;;;;;;;;;;;;;;;;;;;;;;;;;;;;;;;;;;;;;;;;;;;;;;;;;;;;;;;;;;;;;;;;;;;;;;;;;;;;;;;;;;;;;;;;;;;;;;;;
(defun run-lambda (&key (a 1.0) (alpha -1.0) (start-kk 0.0) (end-kk 1.51) (kkstep 0.1))
 (let* ((datafilestr (format nil
                              "LCRIT_a~A_al~A_eps~A_kst~A_kend~A_on_~A_started_~A.data2p1"
                              a alpha
                              eps start-kk end-kk
                                                          (machine-instance) (current-datetime))))

   ;; label columns in output file
   (with-open-file (datafile datafilestr
                              :direction :output
                              :if-exists :supersede)
     (format datafile "kk  lambda-c~%"))

   ;;step through k values and run calc-lambda to find lambda(k)
   (do ((kk start-kk (+ kk kkstep))) ((> kk end-kk))
```

```
131     (format t "eps = ~A kk = ~A lambda = ~A alpha = ~A a = ~A~2%"
132             eps kk llambda alpha a )
133
134     ;;if comp-lambda returns true, write current lambda value as lambdac
135     (setf *lambda-c* (calc-lambda :kk kk :llambda *lambda-c* :alpha alpha :a a))
136
137     ;;print current values of kk, lambda-c to file
138     (with-open-file (datafile datafilestr
139                               :direction :output
140                               :if-exists :append);:supersede)
141       (format datafile "~A ~A~%" kk *lambda-c*))
142     )
143
144   )
145 )
```